Journal of Molecular Liquids 393 (2024) 123537

Contents lists available at ScienceDirect

Journal of Molecular Liquids

journal homepage: www.elsevier.com/locate/molliq

An approach to characterize the nanolayer for a nanofluid: Thickness, density and molar mass

T.P. Iglesias [a,b,*], A. Queirós [a,c], M.F. Coelho [c,d]

[a] Departamento de Física Aplicada, Facultad de Ciencias, Universidad de Vigo, 36310 Vigo, Spain
[b] CINBIO, Universidade de Vigo, 36310 Vigo, Spain
[c] Instituto Superior de Engenharia do Porto, 4200-072 Porto, Portugal
[d] CIETI-Centro de Inovação em Engenharia e Tecnologia Industrial, ISEP, Porto, Portugal

ARTICLE INFO

Keywords:
Nanofluids
Nanolayer
Theoretical models
Density
Alumina

ABSTRACT

The aim of this work is to develop a theoretical approximation to calculate the effective thickness, density and molar mass of the interfacial nanolayer around nanofluid particles. These properties of the nanolayer depend, in general, on temperature, on the nature of the base fluid, the nature of nanoparticles, their geometry and their concentration. The model takes into account all these parameters. This is presented for a general geometry and it is shown that the effective nanolayer molar mass is equal to that of the base fluid. Then, this is particularized for a spherical geometry, which is one of the most usual in literature, and is numerically applied to the aqueous alumina (15 nm) nanofluids at different temperatures and nanoparticle concentrations. The obtained results together with those from the application of the model to some nanofluids from literature, at different temperatures and nanoparticle concentrations, allow providing a general insight into the effective behavior of those nanolayer properties. Finally, it is shown that the model, under its hypothesis, does not support the equation of Pak and Cho except as an approximation.

1. Introduction

The history of humankind has been marked by the discovery and use of new materials. Among the new materials that have arisen in the last quarter century are the nanofluids. These are a type of colloids that consist of solid particles with some of their dimensions between 1 and 100 nm dispersed in a base fluid. The first studies were aimed at developing a new class of heat transfer fluids, in the area of thermal engineering, focusing on the study of the effective thermal conductivity and other properties related to this field. Since then, the experimental and theoretical research of these fluids has attracted the attention of the scientific community due to the unusual behavior of their properties, which is not only of interest from the point of view of their industrial applications but also from the fundamental research standpoint [1,2]. The chronological progress and advances in the field of nanofluids are well documented in the literature, see for example [3–11]. The studies have payed attention to different factors as heat transfer characteristics [3–5,8–11], synthesis methods and stability [6–9,11], particular types of nanofluids [8,11], formulation of thermophysical properties [8], research gaps [9], applications [7] etc.

In order to explain how a small quantity of nanoparticles modifies so significantly the properties of the base fluid, different hypotheses and models have been proposed in the literature. Even though there is no agreement, it seems that one of the accepted hypothesis is that this modification is due to the layer of molecules between the surface of the nanoparticles and the base fluid. In the literature, this interfacial layer at the particle/liquid base interface is known as absorption layer, interfacial layer, interfacial shell or nanolayer, though a more general term from physical chemistry as double layer can be also employed. This layer has different properties from those of the bulk components of the nanofluid. This is the reason why, in general, the theoretical models from the literature consider it as a phase or a different component of the mixture.

Despite all the work carried out in the literature, the properties of the nanolayer, which are essential for determining the effective thermal conductivity of nanofluids, are unknown. The revision presented in [3] provides an overview about its influence on thermo-physical properties of nanofluids. With the aim of obtaining the order of magnitude of the interfacial nanolayer thickness, some authors fitted their experimental values to some theoretical equations of effective thermal conductivity which depends on the interfacial nanolayer thickness. See for example

* Corresponding author at: Departamento de Física Aplicada, Facultad de Ciencias, Universidad de Vigo, 36310 Vigo, Spain.
E-mail address: tpigles@uvigo.es (T.P. Iglesias).

https://doi.org/10.1016/j.molliq.2023.123537
Received 1 September 2023; Received in revised form 24 October 2023; Accepted 7 November 2023
Available online 10 November 2023

Nomenclature

M^*_b	Molar mass of base fluid
M^*_{nl}	Molar mass of nanolayer
M^*_p	Molar mass of nanoparticle
M_m	Molar mass of nanofluid
N_A	Avogadro constant
N_p	Number of nanoparticles
R_p	Nanoparticle radius
R_{pe}	Effective radius of nanoparticle
t	Nanolayer thickness
T	Temperature
V^*_b	Molar volume of base fluid
V^*_i	Molar volume of a component i
V^*_{nl}	Molar volume of nanolayer
V_m	Nanofluid molar volume
V_{nl}	Volume of nanolayer
V_p	Volume of one nanoparticle
V_{pe}	Nanoparticle effective volume
w	Weight fraction
x_i	Mole fraction of a component i
x_{nl}	Molar fraction of nanolayers
x_p	Molar fraction of nanoparticles

Greek symbols

β	Ratio nanoparticle thickness and radius
ΔV_m	Molar volume of mixing
$\Delta\rho$	Deviation of density
ρ	Nanofluid density
ρ_b	Base fluid density
ρ_{nl}	Nanolayer density
ρ_p	Nanoparticle density
ϕ_i	Volume fraction of a component i
ϕ_{nl}	Volume fraction of nanolayers
ϕ_p	Volume fraction of nanoparticles
ϕ_{pe}	Effective volume fraction of the nanoparticles in the mixture

the work of Q. Z. Xue [12] who arrived at thickness of ~ 3 nm for the studied nanofluids. Other authors also consider that the interfacial nanolayer thickness is ~ 1–5 nm. For example, L. Xue et al. [13] supported by experimental and simulation results, consider the thickness of the order of a few atomic distances ~ 1 nm, when simple liquids are used as base fluids. Regarding the explicit equations for calculating the nanolayer thickness, Tillman and Hill [14] derived an expression; however, the approximation requires the knowledge of the functional form of the thermal conductivity in the nanolayer. Wang et al. [15] and Heyhat et al. [16] in their models consider for the nanolayer thickness, t, the Langmuir equation of monolayer adsorption of molecules, $t = 1/\sqrt{3}\left(4M^*_b/\rho_b N_A\right)^{1/3}$, where N_A is Avogadro constant and M^*_b and ρ_b are respectively the molar mass and the density of the base fluid. In this expression, the thickness depends on the temperature through the density of the base fluid, but there is no dependence on the nanoparticle concentration. Langmuir's equation has also been used in the theoretical model of [17] to check some of the results obtained.

As the interfacial nanolayer thickness depends on temperature [3], Sitprasert et al. [18] considering the Leong et al. [19] model for effective thermal conductivity arrive at an explicit equation for nanolayer thickness as a function of temperature, and the nanoparticle radius. Also, Sharifpur et al. [20] considering for spherical nanoparticles that the nanolayer is pure void, give an expression for nanolayer thickness as a polynomial equation of the nanoparticle radius. Tso et al. [21] consider an expression for the thickness that depends on the nanoparticle radius and two parameters, which take particular values depending on the components of the nanofluid. The authors calculate these values for four nanofluids. These equations were deduced for selective nanofluids and specific ranges of nanoparticle concentrations, therefore they are not valid in general.

In this work, an approximation to calculate some effective properties of the interfacial layer, such as thickness, density and molar mass, is proposed. This does not consider its internal structure but only the nanolayer effective properties. This was also considered by Leong et al. [19] in their model for the prediction of the thermal conductivity of nanofluids. In section 2, the model is presented for a general geometry, and it is then particularized for spherical geometry, for which mathematical expressions for nanolayer density and thickness are derived. Then in section 3, the approximation is numerically applied to the aqueous alumina (15 nm) nanofluids at fourteen concentrations (up to 2 % in volume) and at six temperatures (from 293.15 K to 343.15 K). These results together with those obtained from the application of the model to some nanofluids from literature with different base fluids, nanoparticles of different sizes and at different concentrations and temperatures allow providing a general insight into the effective behavior of those nanolayer properties attending to the sign and the magnitude of the molar volume of mixing. As the model considers the effective properties of the nanolayer it does not predict any information about its internal molecular distribution. However, from the prediction of those properties some insights into the internal structure can be provided. For the sake of simplicity, from now on, these effective properties will be named without using the "effective" term.

2. Model

Let us consider a mole of nanofluid of nanoparticles of known composition, and equal geometry and size. The molar fraction, x_p, of the nanoparticles is related to the number of nanoparticles N_p by the following equation:

$$x_p = \frac{N_p V_p}{V^*_p} \tag{1}$$

where V^*_p is the molar volume of the nanoparticles' material and V_p is the volume of one nanoparticle.

A nanofluid is a colloid mixture of two components, however, after carrying out the process of their mixing, it will be considered as a blend of three components: the nanoparticles, the nanolayers and the base fluid. Under this consideration, the nanofluid molar volume, V_m, will be expressed as the sum of the molar volumes of these three components weighted by their respective molar fractions in the mixture:

$$V_m = x_p V^*_p + x_{nl} V^*_{nl} + (1 - x_p - x_{nl}) V^*_b \tag{2}$$

x_{nl} and V^*_{nl} denote respectively the molar fraction and molar volume of the nanolayer, and V^*_b is the molar volume of the base fluid.

Similarly, the molar mass of the nanofluid, M_m, will be expressed as

$$M_m = x_p M^*_p + x_{nl} M^*_{nl} + \left(1 - x_p - x_{nl}\right) M^*_b \tag{3}$$

where M^*_{nl} and M^*_b are the molar masses of the nanolayer and base fluid respectively.

Using equations (2) and (3), the density of the nanofluid, ρ, can be expressed as

$$\rho = \frac{M_m}{V_m} = \frac{x_p M_p^* + x_{nl} M_{nl}^* + (1 - x_p - x_{nl}) M_b^*}{x_p V_p^* + x_{nl} V_{nl}^* + (1 - x_p - x_{nl}) V_b^*} \quad (4)$$

It will be considered the ideal molar volume of a nanofluid as the sum of the molar volumes of the two initial components, nanoparticles and base fluid, weighted by their respective molar fractions, $(1 - x_p)V_b^* + x_p V_p^*$. From equation (2) the deviation of the molar volume from its ideal behavior is given by the following equation

$$\Delta V_m = V_m - \left(x_p V_p^* + (1 - x_p) V_b^*\right) = x_{nl}(V_{nl}^* - V_b^*) \quad (5)$$

following the thermodynamic formalism of liquid mixtures, ΔV_m would be the excess molar volume of the nanofluid. However, in this work it will be named as molar volume of mixing because the conventional excess thermodynamics quantities have not been formally demonstrated for nanofluids. They can only be applied when the mixture and their pure components are homogeneous. In fact, thermodynamics requires that mixture and components should be in the same physical state [22]. Despite these drawbacks, the application of conventional excess thermodynamic quantities to nanofluids is admitted in the literature [18,23–31]. In [31] it is argued the utility of defining the excess electric conductivity for nanofluids and was named as electric conductivity of mixing.

It can be observed in equation (5) that, if $V_{nl}^* > V_b^*$ the nanofluid molar volume of mixing is positive, that is, the molar volume of the nanofluid is larger than what it would be for an ideal behavior. If $V_{nl}^* < V_b^*$, the molar volume of mixing is negative, that is, the nanofluid molar volume is smaller than that of its ideal behavior. It is necessary to take into account that, in both cases, the nanolayer is surrounding the nanoparticle and that ΔV_m will be positive or negative attending to the physicochemical characteristics of the nanolayer. These last will determine the volume of the nanolayer, V_{nl}, that can be calculated with equation (6) below, knowing N_p from equation (1) and admitting that all nanofluid molar volume of mixing comes from the nanolayers:

$$V_{nl} = \frac{|\Delta V_m|}{N_p} = \frac{V_p}{x_p V_p^*} |\Delta V_m| \quad (6)$$

In this expression ΔV_m can be determined from the experimental measure of the density and this is considered in absolute value, to take into account the case in which the physicochemical characteristics of the nanolayer lead to $V_{nl}^* < V_b^*$, see equation (5). In this expression V_p can be known, attending to the nanoparticle geometry, and therefore the nanolayer thickness can also be determined, considering that V_{nl} is homogenously distributed around the nanoparticle. Note that the behavior of V_{nl} with the concentration of the nanoparticles cannot be predicted from equation (6) in a general way, because the dependence of ΔV_m on x_p is characteristic of each nanofluid. In the particular case that $\Delta V_m = 0$, from equation (5), either the molar fraction of the nanolayer is zero, $x_{nl} = 0$, or its molar volume is the same as that of the base fluid , $V_{nl}^* = V_b^*$. In both cases the model predicts that there is no nanolayer.

The addition of the nanolayer volume, V_{nl}, and that of the nanoparticle, V_p, gives the nanoparticle effective volume, V_{pe}:

$$V_{pe} = V_{nl} + V_p \quad (7)$$

therefore, the effective volume fraction of the nanoparticles in the mixture, $\varnothing_{pe}$, is

$$\varnothing_{pe} = \varnothing_{nl} + \varnothing_p \quad (8)$$

where $\varnothing_{nl}$ and $\varnothing_p$ are respectively the volume fractions of the nanolayers and nanoparticles in the nanofluid. Their calculation depends on the geometry of the nanoparticles and is related to the thickness of the nanolayer, t, see Fig. 1. The calculation of $\varnothing_{nl}$ for a spherical geometry is given in section 2.1.

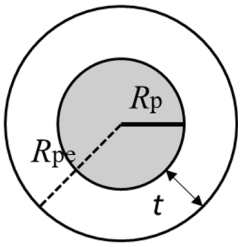

Fig. 1. Representation of a spherical nanoparticle of radius R_p with a nanolayer thickness, t and an effective radius, R_{pe}.

Taking into account the relation between mole fraction and volume fraction in a mixture of these three components, the mole fraction of a component i, x_i, is related to its volume fraction, $\varnothing_i$, by this equation:

$$x_i = \frac{\varnothing_i / V_i^*}{\frac{\varnothing_p}{V_p^*} + \frac{\varnothing_{nl}}{V_{nl}^*} + \frac{1 - \varnothing_p - \varnothing_{nl}}{V_b^*}} \text{ where i = nl or p} \quad (9)$$

From the combination of equations (5) and (9), considering i = nl, the molar volume of the nanolayer can be obtained by the following equation:

$$V_{nl}^* = \frac{\varnothing_{nl}(\Delta V_m + V_b^*)}{\varnothing_{nl} - \Delta V_m \left(\frac{\varnothing_p}{V_p^*} + \frac{1 - \varnothing_p - \varnothing_{nl}}{V_b^*}\right)} \quad (10)$$

The molar mass of the nanolayer can be determined from equation (4) calculating x_{nl} by equation (9), or by equation (5), and if the experimental value of ρ is known:

$$M_{nl}^* = \rho V_{nl}^* + \frac{(1 - x_p - x_{nl})(\rho - \rho_b) V_b^* + x_p (\rho - \rho_p) V_p^*}{x_{nl}} \quad (11)$$

from this equation and considering equation (2) it follows that the nanolayer molar mass is equal to that of the base fluid:

$$M_{nl}^* = M_b^* \quad (12)$$

This more general result for M_{nl}^* than that of equation (11) can also be shown applying the mass conservation before and after mixing in equation (3).

With V_{nl}^* determined by equation (10) and M_{nl}^* from equation (12), the nanolayer density, ρ_{nl}, can be obtained from the equation:

$$\rho_{nl} = \frac{M_{nl}^*}{V_{nl}^*} = \frac{M_b^*}{V_{nl}^*} \quad (13)$$

2.1. Calculation for spherical nanoparticles

As the calculation of t and $\varnothing_{nl}$ depends on the geometry of the nanoparticles, they will be determined in this section for spherical nanoparticles because this geometry is the most usually considered in the nanofluids studied in the literature.

From equations (7) and (6), the effective radius of the nanoparticle, R_{pe}, that is, the radius of the nanoparticle including the nanolayer is given by the following equation:

$$R_{pe} = \left(R_p^3 + \frac{3}{4\pi} V_{nl}\right)^{1/3} = \left(R_p^3 + \frac{3}{4\pi} \frac{V_p}{x_p V_p^*} |\Delta V_m|\right)^{1/3} \quad (14)$$

From this equation the thickness of the nanolayer, t, can be calculated

$$t = R_{pe} - R_p \quad (15)$$

Equations (14) and (15) show that there is a dependence of the nanolayer thickness on the concentration.

Considering the volume of a sphere of radius R_{pe}, Fig. 1, and using equation (15) the effective volume fraction can be calculated:

$$\varnothing_{pe} = (1+\beta)^3 \varnothing_p \tag{16}$$

with

$$\beta = t/R_p \tag{17}$$

and from (8)

$$\varnothing_{nl} = \left[(1+\beta)^3 - 1\right]\varnothing_p \tag{18}$$

Using equation (18) in equation (10) the molar volume of the nanolayer can be calculated, and its density from (13).

Before going to the next section, where these quantities and the nanolayer thickness are calculated for different nanofluids, some considerations about the model proposed above will be examined.

From equations (4) and (9) it is obtained that

$$\rho = \varnothing_p \rho_p^* + \varnothing_{nl}\rho_{nl}^* + (1 - \varnothing_p - \varnothing_{nl})\rho_b^* \tag{19}$$

This equation was admitted by Heyhat et al. [16] in their model of molecular simulation. If in this expression the effect of the nanolayer is disregarded, one arrives at:

$$\rho \cong \varnothing_p \rho_p^* + (1 - \varnothing_p)\rho_b^* \tag{20}$$

This expression was proposed as an approximation to fit the experimental nanofluid density by Pak and Cho in [32]. Various works of the literature, as [33] and [34] have obtained that the magnitude of the deviations, expressed in %, between the experimental values and those obtained by equation (20) for different nanofluids reaches values up to 1.9 % and 8 % respectively.

Following the thermodynamics of liquid mixtures, the right-hand side of this equation would be the expression for the ideal density of the nanofluid. In this equation (20), the equal sign would mean that the system has an ideal behavior, and there would not be interactions between the components of the mixture. This would mean that the nanoparticles would not have a nanolayer, where the most important interactions between the components happen. This result, together with the results of literature mentioned above, shows that the equal sign in equation (20) should in general not be applied.

Another more quantitative way of demonstrating this outcome is as follows. By analogy with the definition given for ΔV_m, the increment of the density, $\Delta\rho$, is defined as the deviation of density from its ideal behavior:

$$\Delta\rho = \rho - \left[\varnothing_p \rho_p^* + (1 - \varnothing_p)\rho_b^*\right] \tag{21}$$

$\Delta\rho$ should not be considered as the excess density of the nanofluid, because the conventional thermodynamic excess quantities are not formally defined for these colloids, as was mentioned above.

$\Delta\rho$ and ΔV_m are related by the following equation, the proof of which is given in the appendix A:

$$\Delta V_m = -\frac{1}{\left(\frac{\varnothing_p}{V_p^*} + \frac{1-\varnothing_p}{V_b^*}\right)}\left[\frac{\Delta\rho}{\rho}\right] \tag{22}$$

If the density of a nanofluid followed the equal sign in equation (20), $\Delta\rho$ would be zero, by equation (21), and by equation (22), $\Delta V_m = 0$. Taking into account equation (6), there would not be nanolayer. That is, the model does not support the equation of Pak and Cho except as an approximation. Indeed, the difference between the equal and approximation signs in equation (20) is what determines $\Delta\rho$. This will be seen quantitatively in section 3.

3. Application to different nanofluids

In order to illustrate and check the model, this was applied to alumina (15 nm) + water using density data measured in our laboratory. We will see the results obtained at the end of this section because in order to obtain more comprehensive information and check the model in more extensive, impartial and trustworthy situations the model was firstly applied to nanofluids from literature. They come from the few published works that provide the size of the nanoparticles, and not a dispersion range of sizes, as well as the numerical values of the density and not only its behavior. These five nanofluids are (A) CuO (11 nm) + water at 283.15 K, 293.15 K and 303.15 K [35]; (B) Si_3N_4 (20 nm) + ethylene glycol at 288.15 K and 298.15 K [36]; (C) TiN (20 or 50 nm) + ethylene glycol at 288.15 K [36] and (D) ZnO (20 nm) + poly (ethylene glycol), PEG 400 at the temperatures of 293.15, 308.15 and 318.15 K [24]. All of them were prepared using the two-step method. System D allowed the study of one case where the sign of the molar volume of mixing changes when the concentration of nanoparticles increases. The values of the densities of the base fluid, ρ_b, and the nanoparticles, ρ_p, necessary to apply the model to these nanofluids are shown in Table 1. All the systems were studied at nanoparticle concentrations below 2 % in volume because this is considered sufficiently low so that nanoparticles act individually to affect the properties of the system [38]. That is, the interactions nanoparticle-nanoparticle can be disregarded in relation to those of nanoparticle-base fluid. Only for the alumina + water system is the maximum concentration of 2 % in volume reached.

(A) *CuO (11 nm) + water.*

In [35], densities of different nanofluids are studied with temperature and pressure. In order to avoid polydispersity, and therefore for a more reliable application of the model, the pressure of one atmosphere and the smallest concentrations of CuO (11 nm) + water (named in [35] sample S2) were chosen. S2 was selected because it presents the lowest radius uncertainty of the samples studied in [35]. The obtained results are shown in Table 2. In [35] the values of density at the different temperatures of the water and that of CuO, necessary to carry out the calculations, are missing. For density of the nanoparticles, the bulk value of 6310 kg m^{-3} [37] was considered at all temperatures. Density of water at the different work temperatures was also obtained from [37].

It can be observed in Table 2 that for this nanofluid the molar volume of mixing is negative. At each temperature, the thickness of the nanolayer decreases with nanoparticle concentration. However, at the same concentration this increases slightly with temperature. This last behavior could be attributed to the thermal agitation. Nanolayer density, ρ_{nl}, is larger than that of the water. It is between the density of the water and that of CuO. It seems that this does not depend on the concentration of the nanoparticles and decreases with temperature. Equation (12) ascertains that its molar mass is equal to that of the base fluid and does not depend on neither temperature nor nanoparticle concentration. As its molar mass coincides with that of the water, the nanolayer could be considered tightly bound water, [38].

(B) *Si_3N_4 (20 nm) + ethylene glycol.*

Table 1
Densities of the base fluids, ρ_b, at different temperatures and bulk density of the nanoparticles, ρ_p

Base fluid				Nanoparticle	ρ_p / kg· m^{-3}
Water [38]					
T/ K	283.15	293.15	303.15	CuO	6310 [37]
ρ_b/ kg·m^{-3}	999.70	998.20	995.65		
Ethylene glycol ($C_2H_6O_2$) [36]					
T/ K	288.15	298.15	308.15	Si_3N_4	3400
ρ_b/ kg·m^{-3}	1116.6	1109.7	1102.7	TiN	5220
PEG 400 ($HO(C_2H_4O)_nH$ [24]					
T/ K	293.15	308.15	318.15	ZnO	5607[a]
ρ_b/ kg·m^{-3}	1126.68	1114.39	1106.21		

[a] Value from the database Scifinder-n

Table 2
Values of molar volume of mixing and the nanolayer properties of thickness, t, molar volume, V^*_{nl} and density, ρ_{nl}, calculated for the nanofluid CuO (11 nm) + water, at different temperatures, T, at the pressure of 0.1 MPa. $M^*_{nl} = 1.801510^{-2}$kg • mol^{-1}by equation (12). Values of nanofluid density, ρ, at the different weight fraction, w, and at the pressure of 0.1 MPa were taken from [35].

w %	ρ kg·m^{-3}	x_p	$\Delta V_m \times 10^8$ m^3·mol^{-1}	t /nm (Eq.15)	$V^*_{nl} \times 10^6$ m^3·mol^{-1} (Eq. 10)	ρ_{nl}/ kg·m^{-3} (Eq. 13)
$T = 283.15$ K						
1	1009.1	0.00228	−1.6336	0.89	9.01	2000
1.75	1015.1	0.00402	−0.8101	0.28	9.01	2000
2.5	1021.3	0.00577	−0.2027	0.05	9.01	2000
$T = 293.15$ K						
1	1007.6	0.00228	−1.6570	0.90	9.02	1997
1.75	1013.6	0.00402	−0.8448	0.29	9.02	1997
2.5	1020.1	0.00577	−0.7791	0.19	9.02	1997
$T = 303.15$ K						
1	1005.2	0.00228	−2.0573	1.08	9.04	1992
1.75	1011.2	0.00402	−1.2627	0.42	9.04	1992
2.5	1017.7	0.00577	−1.2181	0.29	9.04	1992

Table 3 shows the results obtained for Si_3N_4 (20 nm) + ethylene glycol (EG). Reference [36] supplies the values of all the quantities necessary to apply the model. This nanofluid presents positive molar volume of mixing at the studied temperatures. Its nanolayer thickness slightly depends on the temperature. The approximation predicts a very small nanolayer density that changes with the concentration of the nanoparticles. Its molar mass, equation (12), coincides with that of the ethylene glycol ($M^*_{EG} = 6.20710^{-2}$kg·mol^{-1}). As the model considers that the nanolayer is homogenous it cannot give any information about its internal molecular distribution. However, in order to justify those small values of density it could be argue that as this is much smaller than that of EG and its molar mass is that of EG, the interfacial nanolayer could be considered as loosely bound EG, [38]. That is, a small number of molecules of EG loosely weakly bound.

At 288.15 K, Table 3 shows that the nanolayer thickness is between 2.5–1.7 nm, which is ~ 25–17 % of the nanoparticle radius. Therefore, due to the large free intermolecular space in the loosely bound EG molecules (ρ_{nl} is very small) the nanolayer thickness should not be too much affected by the thermal agitation. This agrees with its temperature behavior shown in Table 3 at 288.15 K and 298.15 K.

(C) *TiN (20 and 50 nm) + ethylene glycol.*

The other studied system that presents positive molar volume of mixing is TiN + ethylene glycol [36]. This nanofluid was studied at two nanoparticle sizes, 20 and 50 nm at the temperature of 288.15 K, Table 4. For both nanofluids the nanolayer thickness slightly depends on nanoparticle concentration. The nanolayer density is very small and

Table 3
Values of molar volume of mixing, and the nanolayer properties of thickness, t, density, molar volume, V^*_{nl} and density, ρ_{nl}, calculated for the nanofluid Si_3N_4 (20 nm) + ethylene glycol at different temperatures, T, at the pressure of 0.1 MPa. $M^*_{nl} = 6.20710^{-2}$kg • mol^{-1} by equation (12). Values of nanofluid density, ρ , at the different weight fraction, w, were taken from [36].

w	ρ kg·m^{-3}	x_p	$\Delta V_m \times 10^7$ m^3·mol^{-1}	t / nm (Eq. 15)	$V^*_{nl} \times 10^2$ m^3·mol^{-1} (Eq.10)	ρ_{nl}/ kg·m^{-3} (Eq.13)
$T = 288.15$ K						
0.010	1120.6	0.0044	1.7588	2.5	1.76	3.52
0.025	1130.2	0.0112	2.6814	1.7	1.16	5.36
0.050	1143.4	0.0228	5.7986	1.7	0.54	11.5
$T = 298.15$ K						
0.010	1113.9	0.0044	1.6681	2.4	1.88	3.30
0.025	1123.7	0.0112	2.4854	1.5	1.26	4.91
0.050	1138.2	0.0228	4.9721	1.5	0.63	9.78

Table 4
Values of molar volume of mixing, and the nanolayer properties of thickness, t, molar volume, V^*_{nl} and density, ρ_{nl} calculated for the nanofluid TiN (20 nm or 50 nm) + ethylene glycol at the temperature of 288.15 K and at the pressure of 0.1 MPa. $M^*_{nl} = 6.20710^{-2}$kg • mol^{-1} by equation (12). Values of nanofluid density, ρ, at the different weight fraction, w, were taken from [36].

w	ρ kg·m^{-3}	x_p	$\Delta V_m \times 10^8$ m^3·mol^{-1}	t / nm (Eq. 15)	$V^*_{nl} \times 10^2$ m^3·mol^{-1} (Eq.10)	ρ_{nl}/ kg·m^{-3} (Eq.13)
$R_p = 10$ nm						
0.010	1124.7	0.0100	3.6632	0.94	8.44	0.74
0.025	1137.2	0.0251	8.5468	0.88	3.62	1.71
0.050	1159.8	0.0502	1.1432	0.60	2.71	2.29
$R_p = 25$ nm						
0.010	1125.0	0.0100	2.1915	1.45	14.1	0.44
0.025	1138.0	0.0251	4.7101	1.26	6.57	0.95
0.050	1159.9	0.0502	1.0970	1.45	2.82	2.20

increases with the concentration of the nanoparticles. Using a similar explanation given for the system Si3N4 (20 nm) + ethylene glycol the nanoparticles would be surrounded by a nanolayer of loosely bound EG.

It seems that the size of the nanoparticle has influence on the nanolayer thickness and its density, see Table 4. For $R_p = 25$ nm the thickness is ~ 6 % of the radius while for $R_p = 10$ nm it is ~ 9.5 %. This table also shows that the nanolayer density is larger for the nanofluid with smaller nanoparticle size. That is, the nanolayer density and the ratio t/R_p are larger for the nanofluid with smaller nanoparticle size.

(D) *ZnO (20 nm) + PEG 400.*

For this nanofluid, [24], the molar volume of mixing changes sign from negative to positive when the nanoparticle concentration is increased. The sign change happens at largest concentrations when temperature increases, Fig. 2. At 293.15 K, the three largest concentrations present $\Delta V_m > 0$, while this happens only for the largest concentration at 318. 15 K, see Fig. 2. Regarding the behavior of the density, Fig. 3a shows its dependence on the nanoparticle volume fraction. The behavior is linear, but this was represented in a logarithmic scale in order to show better the behavior at low concentrations. The good visual fit between the experimental points and the line that represents equation (20) might lead one to think that the nanofluid follows an ideal behavior. In order to clarify this behavior, the increment of the density, $\Delta\rho$, was determined. In Fig. 3b the nanoparticle volume fraction dependence of $\Delta\rho$ at the three temperatures is represented. The behaviors of $\Delta V_m \neq 0$ and $\Delta\rho \neq 0$ from Figs. 2 and 3b show that the nanofluid does not present ideal behavior. This conclusion cannot be obtained directly from the behavior of ρ in Fig. 3a.

Fig. 4 shows that when $\Delta V_m < 0$ the nanolayer thickness increases with the temperature (possibly due to thermal agitation) and decreases with the molar fraction. Only for the largest concentration, which shows

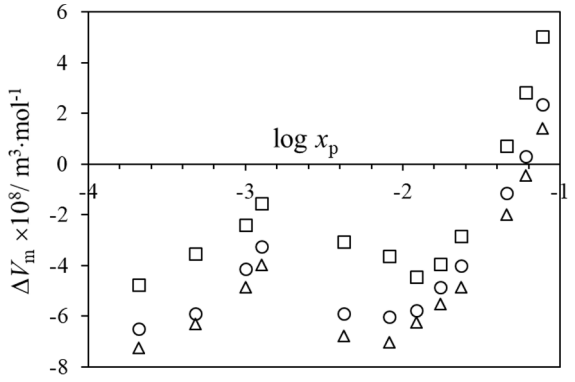

Fig. 2. Nanoparticle molar fraction dependence of molar volume of mixing, ΔV_m, for ZnO (20 nm) + PEG 400 nanofluid at temperatures of 293.15 K, □; 308.15 K, o; 318.15 K, Δ.

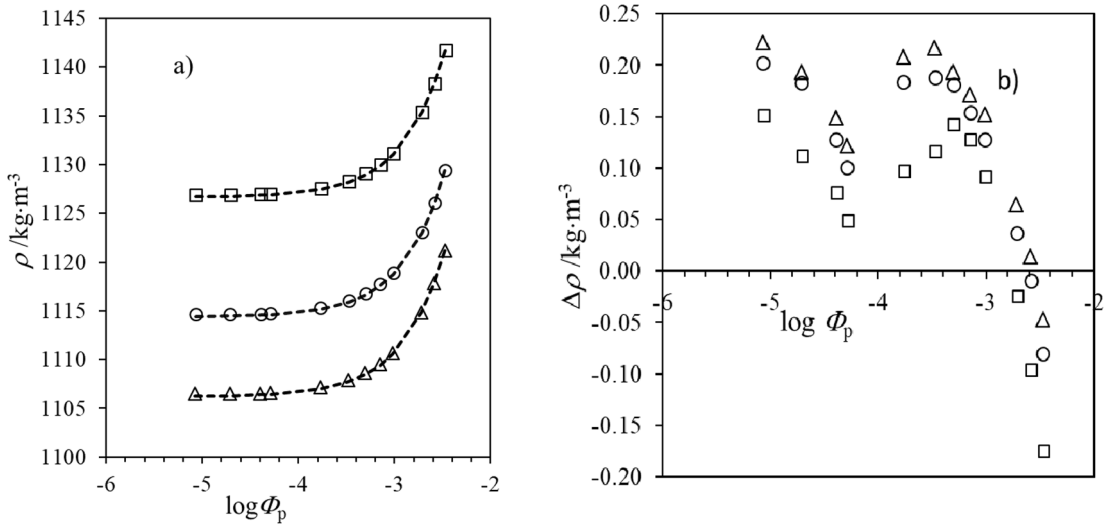

Fig. 3. Nanoparticle volume fraction dependence of a) density, ρ; b) increment of the density, $\Delta\rho$ equation (21), for ZnO (20 nm) + PEG 400 nanofluid at temperatures of 293.15 K, □; 308.15 K, o; 318.15 K, Δ.

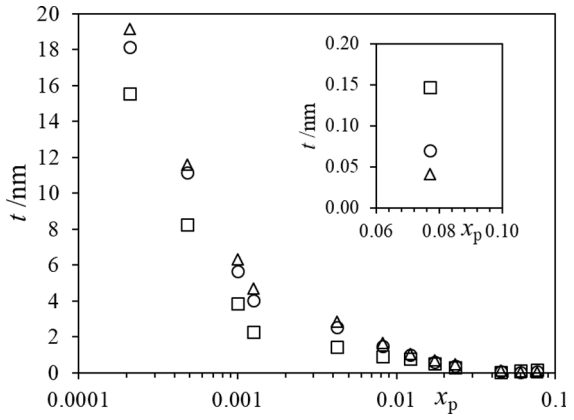

Fig. 4. Nanoparticle molar fraction dependence of nanolayer thickness, t, for ZnO (20 nm) + PEG 400 nanofluid at temperatures of 293.15 K, □; 308.15 K, o; 318.15 K, Δ. In the inset, this dependence is shown for the only concentration that presents $\Delta V_m > 0$ at the three temperatures.

$\Delta V_m > 0$ at the three temperatures, the interfacial nanolayer decreases with temperature. This case is showed in the inset of the figure. Following a similar reasoning to that given for the other nanofluids studied above, when $V_m^E < 0$ the nanolayer density $\rho_{nl} > \rho_{PEG}$ and the nanolayer molar mass $M_{nl}^* = M_{PEG}^*$, therefore the interfacial nanolayer thickness is tightly bound PEG. When $V_m^E > 0$, the nanolayer density $\rho_{nl} \ll \rho_{PEG}$ and the molar mass $M_{nl}^* = M_{PEG}^*$, therefore, the interfacial nanolayer thickness could be considered loosely bound PEG.

Fig. 5 shows that when $\Delta V_m < 0$ the nanolayer density is larger than that of the PEG400. It does not depend on the nanoparticle concentration and it does so only slightly on the temperature. However, when $\Delta V_m > 0$, this density increases with concentration and decreases with the temperature.

As discussed concerning Fig. 2, since there is a change in the sign of the molar volume of mixing, there should be a molar fraction at which $\Delta V_m = 0$. For that value, as it was mentioned above, there is no nanolayer and the system has an ideal behavior. It seems that at these relatively high concentrations (x_p or order 0.1) the nanolayer thickness is so small that it might mean that the system is not sufficiently stable. This case would require a deep experimental study for a more formal clarification, studying experimentally the density in the range of concentrations for which ΔV_m tends to zero.

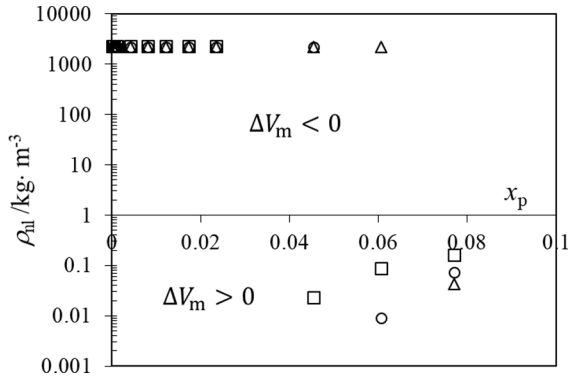

Fig. 5. Nanoparticle molar fraction dependence of nanolayer density,ρ_{nl}, for ZnO (20 nm) + PEG 400 nanofluid at temperatures of 293.15 K, □; 308.15 K, o; 318.15 K, Δ.

(E) *Al_2O_3 (15 nm) + water.*

The density of this nanofluid was measured in our laboratory at fifteen concentrations (up to 2 % in volume) and at six temperatures (from 293.15 K to 343.15 K). Samples of 50 ml were prepared by weight. Al_2O_3 (15 nm) nanopowder 99.5 % pure was supplied by MKnano. The samples were homogenized with 10 min of magnetic agitation followed by intensive ultrasound vibration from a Bandelin Sonopuls HD2200 apparatus equipped with a titanium flat tip TT 13 of 13 mm diameter. The measure of the density was carried out using a conical-shaped pycnometer. A PolyScience 9102A12E circular bath was used for its temperature control. After the bath stabilized at each desired temperature, the pycnometer was maintained immersed 10 min in the bath, to ensure a uniform temperature of the sample. The uncertainty of the temperature was of 0.01 K. Several weightings of the pycnometer were made under the same conditions until a concordant value was obtained between them [39]. They were performed on a Mettler AT-201 balance, with a reproducibility between 0.015 and 0.03 mg and an uncertainty of ± 0.0001 g. The pycnometer was previously calibrated with Milli-Q water and their density values at the temperatures in study were taken from [40]. The estimated uncertainty in the density measurements is $4{\cdot}10^{-4}$ g·cm^{-3}. The experimental densities at the different concentrations and temperatures are in Table 5. The uncertainty of the experimental procedure at the lower concentrations of the temperatures of 293.15 and 303.15 K is not able to distinguish the influence in ρ of change in x_p. The

Table 5
Densities of the nanofluid Al_2O_3 (15 nm) + water at different concentrations and temperatures at the atmospheric pressure of 102 kPa.

T/ K	293.15	303.15	313.15	323.15	333.15	343.15
x_p				ρ / kg· m^{-3}		
0.00012	–	–	993.8	991.1	988.5	985.2
0.00020	–	–	994.6	993.0	989.9	988.1
0.00027	–	996.4	995.1	993.5	990.8	989.1
0.00032	999.8	996.6	995.4	993.7	991.2	989.4
0.00099	1001.4	999.2	998.2	996.0	993.9	992.0
0.00171	1004.2	1002.0	1000.5	998.6	996.7	994.9
0.00263	1007.7	1005.6	1003.8	1002.2	1000.2	998.4
0.00325	1010.1	1008.0	1006.2	1004.5	1002.5	1000.8
0.00493	1016.6	1014.5	1012.5	1011.1	1009.1	1007.2
0.00661	1023.1	1021.0	1019.0	1017.5	1015.6	1013.9
0.00809	1028.8	1026.8	1024.5	1023.3	1021.3	1019.5
0.00984	1035.6	1033.5	1031.3	1030.0	1028.0	1026.5
0.01160	1042.4	1040.4	1037.8	1037.0	1034.9	1033.2
0.01315	1048.4	1046.5	1043.8	1042.7	1040.7	1039.3

Standard uncertainties u are $u(T) = 0.01$ K, $u(x_p) = 10^{-5}$, $u(\rho) = 0.4$ kg· m^{-3}, $u(p) = 1$ kPa

considered density values of the base fluid and nanoparticles necessary to calculate the numerical values of $\Delta\rho$ and ΔV_m as well as ρ_{nl}, t and V^*_{nl} are provided in Table 6. Those calculated values can be found in the support material.

Fig. 6 shows that ΔV_m is negative for the temperatures between 323.15 and 343.15 K. It changes sign from negative to positive at 313.15 K and it is positive at all studied concentrations at the temperatures of 293.15 and 303.15 K. The Figs. 6 and 7 show that $\Delta V_m \neq 0$ and $\Delta\rho \neq 0$, that is, these nanofluids do not follow an ideal behavior and therefore the equation of Pak and Cho is not applicable.

Regarding the behavior of nanolayer thickness, t, this decreases with the concentration, Fig. 8, except at 313.15 K around the molar fraction concentration for which ΔV_m changes sign. The thickness decreases with temperature when $\Delta V_m > 0$, Fig. 8a, that is, when the nanolayer becomes less dense with temperature, Fig. 9, and increases with temperature when $\Delta V_m < 0$, Fig. 8b, that is, when the nanolayer density decreases very slightly with temperature, Fig. 9 and support material.

The behavior of the nanofluid at 313.15 K deserves special attention because, around a molar fraction of 0.005, ΔV_m changes its sign from negative to positive, Fig. 6. At this temperature, t decreases with concentration while $\Delta V_m > 0$ but increases around that concentration when $\Delta V_m < 0$, see Fig. 8a. It seems that there could be a concentration at which $\Delta V_m = 0$. For this concentration there would be no nanolayer as it happens around a concentration of 0.05 for the system D studied above.

4. Conclusions

In a nanofluid the interactions between nanoparticles and their environment change the properties of their surrounding volume, named nanolayer, affecting the material performance. In this work, a model is proposed that allows the estimation of the interfacial nanolayer thickness, its density, and its molar mass. This assumes that the whole molar volume of mixing comes from the interfacial nanolayer thickness. That is, it is considered that the whole molar volume of mixing comes from the interactions between nanoparticles and base fluid. It is admitted in literature that nanoparticle concentrations below 2 % in volume are sufficiently low so that nanoparticles act individually to affect the properties of the system [38]. This 2 % in volume would be the limit in concentration for which the nanoparticle-nanoparticle interactions can be disregarded and therefore the model can be applied. Regardless of this restriction, the approximation is valid for any nanofluid as long as the nanoparticle geometry and the molar volume of mixing are known.

The nanolayer properties studied in this work depend, in general, on temperature, nature of base fluid, nature of nanoparticles, and their geometry and concentration, because of the dependence of ΔV_m on these quantities. This represents an advantage over the models of the literature for the calculation of the nanolayer thickness (see the introduction) which are empirical or do not take into account its dependence on all these quantities. Also, to the best of the authors' knowledge this is the first model that allows the calculation of the effective density, thickness and molar mass of the nanolayer in terms of nanoparticle concentration and temperature. A study of the empirical equation of Pak and Cho was performed. It is shown that the model, under its hypothesis, does not support this equation except as an approximation.

The model was applied to nanofluids with spherical geometry and at different concentrations and temperatures. As the model considers that

Table 6
Densities of the water base fluid,ρ_b, at the temperatures of table 5 and bulk density of the Al_2O_3 nanoparticles,ρ_p.

Water		Al_2O_3
T/ K	ρ_b / kg· m^{-3} [40]	ρ_p / kg· m^{-3}
293.15	998.20	3700 [a]
303.15	995.65	
313.15	992.22	
323.15	988.04	
333.15	983.20	
343.15	977.77	

[a] Value from the provider.

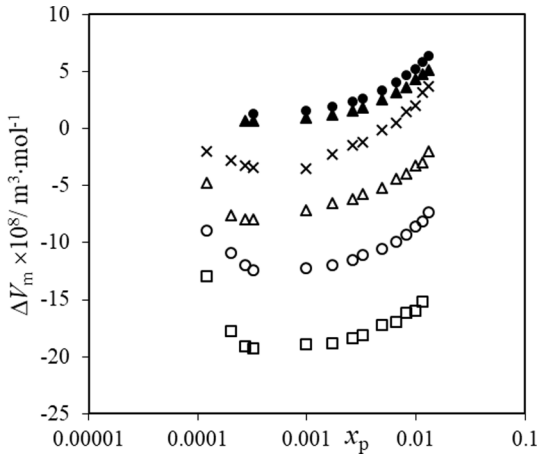

Fig. 6. Nanoparticle molar fraction dependence molar volume of mixing, ΔV_m, for Al_2O_3 (15 nm) + water at the temperatures of 293.15 K, filled circles; 303.15 K, filled triangles; 313.15 K, ×; 323.15 K, Δ; 333.15 K, o; 343.15 K, □.

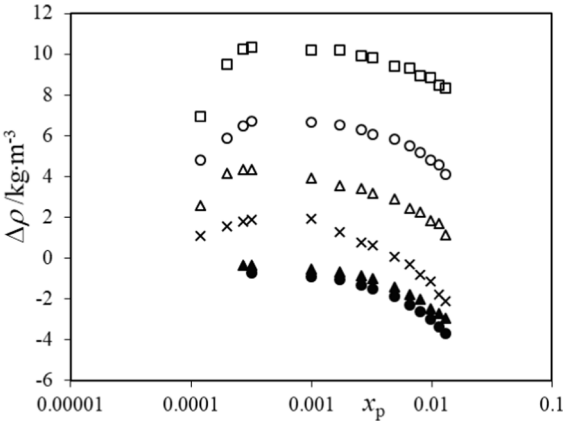

Fig. 7. Nanoparticle molar fraction dependence of the increment of the density, $\Delta\rho$, for Al_2O_3 (15 nm) + water at the temperatures of 293.15 K, filled circles; 303.15 K, filled triangles; 313.15 K, ×; 323.15 K, Δ; 333.15 K, o; 343.15 K, □.

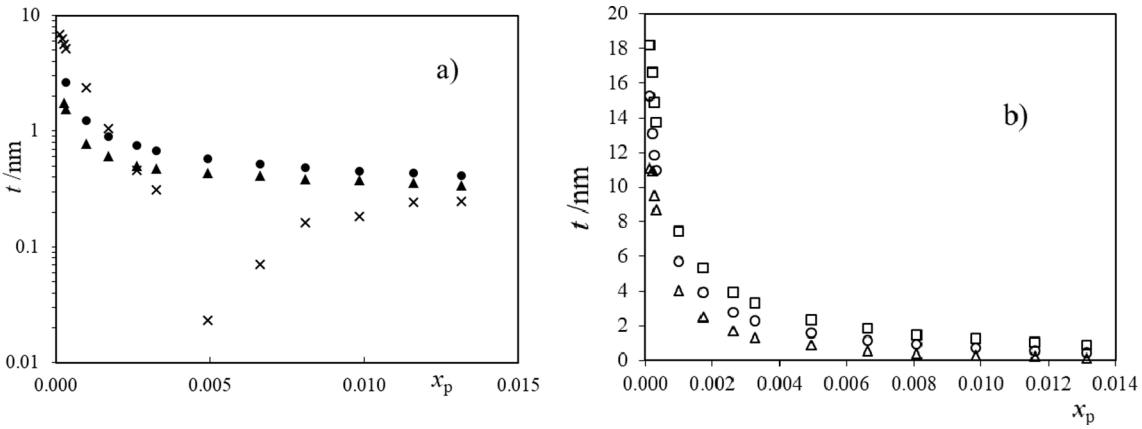

Fig. 8. Nanoparticle molar fraction dependence of the nanolayer thickness, t, for Al_2O_3 (15 nm) + water at the temperatures of: a) 293.15 K, filled circles; 303.15 K, filled triangles; 313.15 K, ×; b) 323.15 K, Δ; 333.15 K, o; 343.15 K, □.

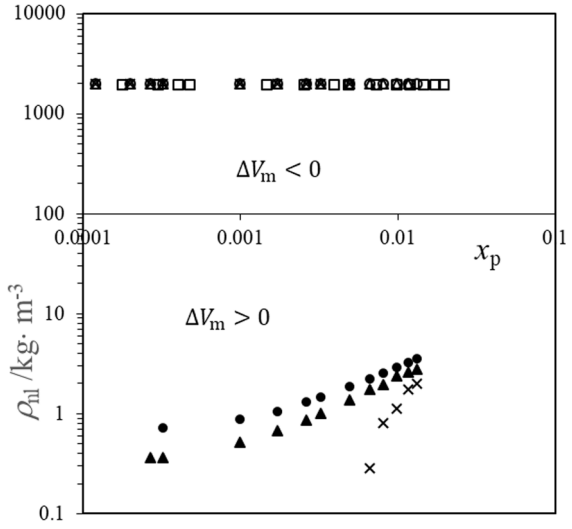

Fig. 9. Nanoparticle molar fraction dependence of the nanolayer density, ρ_{nl}, for Al_2O_3 (15 nm) + water at the temperatures of 293.15 K, filled circles; 303.15 K, filled triangles; 313.15 K, ×; 323.15 K, Δ; 333.15 K, o; 343.15 K, □.

the nanolayer is homogenous it cannot give concrete information about its internal molecular distribution. However, some hints can be obtained from the effective properties. Attending to the sign of ΔV_m the results can be summarized as follows. For the systems that present $\Delta V_m < 0$: (a) the nanolayer thickness increases with temperature and decreases with nanoparticle concentration; (b) nanolayer density value is between those of the bulk nanoparticles and base fluid; (c) nanolayer density decreases with temperature and tends to remain unchanged with nanoparticle concentration. To explain this behavior, and taking into account that $M^*_{nl} = M^*_b$ the interfacial nanolayer could be considered as tightly bound base fluid. When $\Delta V_m > 0$ the following different behavior was found: (a) the nanolayer thickness decreases both with temperature and with nanoparticle concentration; (b) nanolayer density is very small when is compared to that of the bulk nanoparticles or base fluid; (c) nanolayer density increases with nanoparticle concentration and decreases with temperature. To justify this behavior and taking into account that $M^*_{nl} = M^*_b$ the nanolayer could be considered as loosely bound base fluid. The special limit of $\Delta V_m = 0$ is a singular case that needs a separate treatment, with deeper experimental study and a dedicated formal analysis.

Attending to the behavior with temperature and concentration, the following interpretation, could be given for the obtained results. Changing temperature and keeping constant the nanoparticle concentration, when $\Delta V_m < 0$, the system contracts, the nanolayer becomes smaller and therefore will have a larger density than that of the base fluid. This would mean that nanoparticles have a larger interaction with the molecules near their surfaces, the molecules of the nanolayers, than in the ideal case. At such higher density, thermal agitation would slightly reduce the interactions with the farthest molecules of the nanolayer and would lead to an increment of the nanolayer thickness reducing slightly its density. In the case $\Delta V_m > 0$ the opposite would happen. When system expands, each nanolayer would have a smaller density than that of the base fluid. This would mean that the nanoparticle would have a weaker interaction with the molecules near its surface and perhaps much weaker with those of the nanolayer more distant. These molecules would lose the interaction with the nanoparticle because of the thermal agitation and therefore the nanolayer thickness would reduce and density would increase.

At constant temperature, independently of the sign of ΔV_m, the nanolayer thickness decrease with the increment of the nanoparticle concentration. This happens independently of whether the concentration is very low or near of the 2 % mentioned above, see the system alumina + water. This could be explained considering that as x_p increases, the number of nanoparticles in the base fluid increases. Accordingly, there are fewer molecules of the base fluid per nanoparticle. Each nanoparticle would have a smaller number of molecules of base fluid to be controlled because its interaction with the molecules of the base fluid around it would be more easily neutralized by the interactions from the nearer nanoparticles randomly distributed.

It remains, as an open issue, the application of the model to other nanoparticle geometries and the prediction of other thermophysical properties of the nanolayer, as for example its thermal conductivity. Regarding this quantity there are different models in the literature, see for example some of them in [8,10], which from the experimental values and the knowledge of the nanolayer thickness would allow its determination. This knowledge can be important because the nanolayer affects the thermal conductivity through the simple conduction liquid / nanoparticle interface. It also affects the translational thermal energy and convection in the base fluid due to the Brownian motion. The information provided in this work may allow elucidating the importance of those mechanisms, simple conduction and Brownian motion. However, this would require a deeper study.

Apart of their importance in the field of thermal engineering in the sense mentioned above, the results obtained in this work could also be of interest concerning the stability with respect to nanoparticle concentration. In both cases, $\Delta V_m < 0$ and $\Delta V_m > 0$, the nanolayer thickness decreases with nanoparticle concentration. If the stability of the nanofluids were related to the size of the nanolayer, the results obtained for the nanofluids studied in this work suggest the possibility that the

system could become more unstable with the increment of the nanoparticle molar fraction. Broadly speaking, this work tries to contribute to the knowledge of the nanolayer properties because their control could be important in the development of nano and micro technologies, [14], or more in general in the field of colloids, [38].

Summarizing, this work offers a practical model to quantitatively predict the nanolayer thickness and nanolayer density as a function of temperature and parameters of the nanofluid constituents, including base density and nanoparticle concentration. The model predicts only effective quantities, but it can shed some light on the microscopic characteristics of the nanolayer. Finally, it opens an avenue to further studies.

CRediT authorship contribution statement

T.P. Iglesias: Conceptualization, Methodology, Formal analysis, Writing – original draft, Writing – review & editing. **A. Queirós:** Validation, Investigation, Writing – review & editing. **M.F. Coelho:** Validation, Investigation, Writing – review & editing.

Declaration of Competing Interest

The authors declare that they have no known competing financial interests or personal relationships that could have appeared to influence the work reported in this paper.

Data availability

Data will be made available on request.

Acknowledgements

T.P. I. acknowledges the financial support by the grants ED431C 2020-06 provided by the Xunta de Galicia (Spain) and the European Union project H2020-MSCA-RISE-2019 PEPSA-MATE (project number 872233).

Appendix A

Demonstration of equation (22).

From equation (5), the molar volume of mixing obeys

$$\Delta V_m = V_m - \left(x_p V_p^* + (1-x_p) V_b^*\right) \tag{A1}$$

$$\Delta V_m = \frac{M_m}{\rho} - \left(x_p \frac{M_p}{\rho_p} + (1-x_p)\frac{M_b}{\rho_b}\right) \tag{A2}$$

Taking into account the relation between molar fraction, x_p and volume fraction, $\varnothing_p$, (see equation (9) with i = p and $\varnothing_{nl} = 0$)

$$x_p = \frac{\varnothing_p / V_p^*}{\frac{\varnothing_p}{V_p^*} + \frac{1-\varnothing_p}{V_b^*}} \tag{A3}$$

It is obtained that

$$\Delta V_m = \frac{M_m}{\rho} - \left(\frac{\varnothing_p}{\frac{\varnothing_p}{V_p^*} + \frac{1-\varnothing_p}{V_b^*}} + \frac{(1-\varnothing_b)}{\frac{\varnothing_p}{V_p^*} + \frac{1-\varnothing_p}{V_b^*}}\right) = \frac{M_m}{\rho} - \frac{1}{\frac{\varnothing_p}{V_p^*} + \frac{1-\varnothing_p}{V_b^*}} \tag{A4}$$

For the molar mass, M_m, one has

$$M_m = x_p M_p^* + (1-x_p) M_b^* = \frac{\varnothing_p \bullet \rho_p}{\left(\frac{\varnothing_p}{V_p^*} + \frac{1-\varnothing_p}{V_b^*}\right)} + \frac{(1-\varnothing_p)\rho_p}{\left(\frac{\varnothing_p}{V_p^*} + \frac{1-\varnothing_p}{V_b^*}\right)} = \frac{\varnothing_p \bullet \rho_p + (1-\varnothing_p)\rho_p}{\left(\frac{\varnothing_p}{V_p^*} + \frac{1-\varnothing_p}{V_b^*}\right)} \tag{A5}$$

Dividing (A5) by ρ and using this results in (A4):

$$\Delta V_m = \frac{\varnothing_p \bullet \rho_p + (1-\varnothing_p)\rho_p}{\rho\left(\frac{\varnothing_p}{V_p^*} + \frac{1-\varnothing_p}{V_b^*}\right)} - \frac{1}{\frac{\varnothing_p}{V_p^*} + \frac{1-\varnothing_p}{V_b^*}} = -\frac{1}{\left(\frac{\varnothing_p}{V_p^*} + \frac{1-\varnothing_p}{V_b^*}\right)} \frac{\left[\rho - (\varnothing_p \bullet \rho_p + (1-\varnothing_p)\rho_p\right]}{\rho} = -\frac{1}{\left(\frac{\varnothing_p}{V_p^*} + \frac{1-\varnothing_p}{V_b^*}\right)} \left[\frac{\Delta\rho}{\rho}\right] \tag{A6}$$

Appendix B. Supplementary material

Supplementary data to this article can be found online at https://doi.org/10.1016/j.molliq.2023.123537.

References

[1] E.L. Wolf, Nanophysics and nanotechnology: an introduction to modern concepts in nanoscience, second ed., Wiley-VCH, Weinheim, 2006.

[2] S.M.S. Murshed and C.A. Nieto de Castro, editors, Nanofluids: synthesis, properties, and applications, Nova Science, cop., New York, 2014.

[3] J.A. Eastman, S.R. Phillpot, S.U.S. Choi, P. Keblinski, Thermal transport in nanofluids, Annu. Rev. Mater. Res. 34 (2004) 219–246, https://doi.org/10.1146/annurev.matsci.34.052803.090621.

[4] V. Trisaksri, S. Wongwises, Critical review of heat transfer characteristics of nanofluids, Renew. Sust. Energ. Rev. 11 (2007) 512–523, https://doi.org/10.1016/j.rser.2005.01.010.

[5] X.Q. Wang, A.S. Mujumdar, Heat transfer characteristics of nanofluids: a review, Int. J. Therm. Sci. 46 (2007) 1–19, https://doi.org/10.1016/j.ijthermalsci.2006.06.010.

[6] A. Ghadimi, R. Saidur, H.S.C. Metselaar, A review of nanofluid stability properties and characterization in stationary conditions, Int. J. Heat Mass Transf. 54 (2011) 4051–4068, https://doi.org/10.1016/j.ijheatmasstransfer.2011.04.014.

[7] R. Taylor, S. Coulombe, T. Otanicar, P. Phelan, A. Gunawan, W. Lv, G. Rosengarten, R. Prasher, H. Tyagi, Small particles, big impacts: A review of the diverse applications of nanofluids, J. Appl. Phys. 113 (2013) 011301 (19pp). http://doi.org/10.1063/1.4754271.

[8] K.S. Suganthi, K.S. Rajan, Metal oxide nanofluids: Review of formulation, thermo-physical properties, mechanisms, and heat transfer performance, Renew. Sust. Energ. Rev. 76 (2017) 226–255, https://doi.org/10.1016/j.rser.2017.03.043.

[9] N. Sezer, M.A. Atieh, M. Koç, A comprehensive review on synthesis, stability, thermophysical properties, and characterization of nanofluids, Powder Technol. 344 (2019) 404–431, https://doi.org/10.1016/j.powtec.2018.12.016.

[10] L. Qiu, N. Zhu, Y. Feng, E.E. Michaelides, G. Żyła, D. Jing, X. Zhang, P.M. Norris, C. N. Markides, O. Mahian, A review of recent advances in thermophysical properties at the nanoscale: From solid state to colloids, Phys. Rep. 843 (2020) 1–81, https://doi.org/10.1016/j.physrep.2019.12.001.

[11] D. Yadav, M. Sanserwal, A comprehensive review of the effects of various factors on the thermal conductivity and rheological characteristics of CNT nanofluids, J. Therm. Anal. Calorim. 148 (2023) 1723–1763, https://doi.org/10.1007/s10973-022-11821-7.

[12] Q.Z. Xue, Model for effective thermal conductivity of nanofluids, Phys. Lett. A 307 (2003) 313–317, https://doi.org/10.1016/S0375-9601(02)01728-0.

[13] L. Xue, P. Keblinski, S.R. Phillpot, S.-U.-S. Choi, J.A. Eastman, Effect of liquid layering at the liquid–solid interface on thermal transport, Int. J. Heat Mass Transf. 47 (2004) 4277–4284, https://doi.org/10.1016/j.ijheatmasstransfer.2004.05.016.

[14] P. Tillman, J.M. Hill, Determination of nanolayer thickness for a nanofluid, Int. Commun. Heat Mass Transf. 34 (2007) 399–407, https://doi.org/10.1016/j.icheatmasstransfer.2007.01.011.

[15] B. Wang, L. Zhou, X. Peng, A fractal model for predicting the effective thermal conductivity of liquid with suspension of nanoparticles, Int. J. Heat Mass Transf. 46 (2003) 2665–2672, https://doi.org/10.1016/S0017-9310(03)00016-4.

[16] M.M. Heyhat, M. Abbasi, A. Rajabpour, Molecular dynamic simulation on the density of titanium dioxide and silver water-based nanofluids using ternary mixture model, J. Mol. Liq. 333 (2021), 115966, https://doi.org/10.1016/j.molliq.2021.115966.

[17] W. Cui, Z. Shen, J. Yang, S. Wu, Modified Prediction model for thermal conductivity of spherical nanoparticle suspensions (nanofluids) by introducing static and dynamic mechanisms, Ind. Eng. Chem. Res. 53 (2014) 18071–18080, https://doi.org/10.1021/ie503296g.

[18] C. Sitprasert, P. Dechaumphai, V. Juntasaro, A thermal conductivity model for nanofluids including effect of the temperature-dependent interfacial layer, J. Nanopart. Res. 11 (2009) 1465–1476, https://doi.org/10.1007/s11051-008-9535-4.

[19] K.C. Leong, C. Yang, S.M.S. Murshed, A model for the thermal conductivity of nanofluids – the effect of interfacial layer, J. Nanopart. Res. 8 (2006) 245–254, https://doi.org/10.1007/s11051-005-9018-9.

[20] M. Sharifpur, S. Yousefi, J. Yousefi, J.P. Meyer, A new model for density of nanofluids including nanolayer, Int. Commun. Heat Mass Transf. 78 (2016) 168–174, https://doi.org/10.1016/j.icheatmasstransfer.2016.09.010.

[21] C.Y. Tso, S.C. Fu, C.Y.H. Chao, A semi-analytical model for the thermal conductivity of nanofluids and determination of the nanolayer thickness, Int. J. Heat Mass Transf. 70 (2014) 202–214, https://doi.org/10.1016/j.ijheatmasstransfer.2013.10.077.

[22] R. Privat, J.-N. Jaubert, Discussion around the paradigm of ideal mixtures with emphasis on the definition of the property changes on mixing, Chem. Eng. Sci. 82 (2012) 319–333, https://doi.org/10.1016/j.ces.2012.07.030.

[23] S.M. Hosseini, M.M. Alavianmehr, J. Moghadasi, Application of perturbed hard-sphere equation of state to the study of volumetric properties of nano-fluids, Fluid Phase Equilib. 423 (2016) 181–189, https://doi.org/10.1016/j.fluid.2016.04.026.

[24] M.T. Zafarani-Moattar, R. Majdan-Cegincara, Effect of temperature on volumetric and transport properties of nanofluids containing ZnO nanoparticles poly(ethylene glycol) and water, J. Chem. Thermodyn. 54 (2012) 55–67, https://doi.org/10.1016/j.jct.2012.03.010.

[25] M.J. Pastoriza-Gallego, L. Lugo, D. Cabaleiro, J.L. Legido, M.M. Piñeiro, Thermophysical profile of ethylene glycol-based ZnO nanofluids, J. Chem. Thermodyn. 73 (2014) 23–30, https://doi.org/10.1016/j.jct.2013.07.002.

[26] C. Wei, Z. Nan, X. Wang, Z. Tan, Investigation on Thermodynamic Properties of a Water-Based Hematite Nanofluid, J. Chem. Eng. Data 55 (2010) 2524–2528, https://doi.org/10.1021/je900883j.

[27] T.P. Iglesias, M.A. Rivas, R. Iglesias, J.C.R. Reis, F. Coelho, Electric permittivity and conductivity of nanofluids consisting of 15 nm particles of alumina in base Milli-Q and Milli- Ro water at different temperatures, J. Chem. Thermodyn. 66 (2013) 123–130, https://doi.org/10.1016/j.jct.2013.06.019.

[28] R. Iglesias, M.A. Rivas, J.C.R. Reis, T.P. Iglesias, Permittivity and electric conductivity of aqueous alumina (40 nm) nanofluids at different temperatures, J. Chem. Thermodyn. 89 (2015) 189–196, https://doi.org/10.1016/j.jct.2015.05.021.

[29] M.F. Coelho, M.A. Rivas, G. Vilão, E.M. Nogueira, T.P. Iglesias, Permittivity and electrical conductivity of copper oxide nanofluid (12 nm) in water at different temperatures, J. Chem. Thermodyn. 132 (2019) 164–173, https://doi.org/10.1016/j.jct.2018.12.025.

[30] M.F. Coelho, M.A. Rivas, E.M. Nogueira, T.P. Iglesias, Permittivity of (40 nm and 80 nm) alumina nanofluids in ethylene glycol at different temperatures, J. Chem. Thermodyn. 158 (2021), 106423, https://doi.org/10.1016/j.jct.2021.106423.

[31] T.P. Iglesias, C.R. João, Reis,, On the definition of excess electrical conductivity, J. Mol. Liq. 344 (2021), 117764, https://doi.org/10.1016/j.molliq.2021.117764.

[32] B.C. Pak, Y.I. Cho, Hydrodynamic and heat transfer study of dispersed fluids with submicron metallic oxide particles, Exp. Heat Transf. 11 (1998) 151–170, https://doi.org/10.1080/08916159808946559.

[33] J.I. Prado, J.P. Vallejo, L. Lugo, A new relationship on transport properties of nanofluids, Evidence with Novel Magnesium Oxide Based n-Tetradecane Nanodispersions, Powder Technol. 397 (2022), 117082, https://doi.org/10.1016/j.powtec.2021.117082.

[34] R.S. Vajjha, D.K. Das, B.M. Mahagaonkar, Density measurement of different Nanofluids and their comparison with theory, Pet. Sci. Technol. 27 (2009) 612–624, https://doi.org/10.1080/10916460701857714.

[35] M.J. Pastoriza-Gallego, C. Casanova, J.L. Legido, M.M. Piñeiro, CuO in water nanofluid: Influence of particle size and polydispersity on volumetric behaviour and viscosity, Fluid Phase Equilib. 300 (2011) 188–196, https://doi.org/10.1016/j.fluid.2010.10.015.

[36] G. Zyla, J.P. Vallejo, L. Lugo, Isobaric heat capacity and density of ethylene glycol based nanofluids containing various nitride nanoparticle types: An experimental study, J. Mol. Liq. 261 (2018) 530–539, https://doi.org/10.1016/j.molliq.2018.04.012.

[37] D. R. Lide, Handbook of Chemistry and Physics, eightieth ed., CRC Press Boca Raton, London, New York, and Washington DC, 1999-2000.

[38] John C. Berg, An introduction to Interface and Colloids. The bridge to nanoscience, 2010, World Scientific, New Jersey. ISBN-13 978–981-4293-07-5.

[39] Y. Zhang, J. Yang, B. Li, R. Zhang, X. Xie, J. Zhang, Density, viscosity, and spectroscopic and computational analyses for hydrogen bonding interaction of 1,2-propylenediamine and ethylene glycol mixtures, J. Mol. Liq. 302 (2020), 112443, https://doi.org/10.1016/j.molliq.2020.112443.

[40] R.H. Perry, Perry's Chemical Engineers' Handbook, 7th edition, McGraw-Hill, USA, 1997.